8

Assembly and Welding Processes and Their Monitoring and Control

S. Jack Hu
University of Michigan

Elijah Kannatey-Asibu, Jr.
University of Michigan

Assembly is a very important part of most product realization processes. Components fabricated through machining, forming, etc. will be assembled together to form higher level of assemblies or the final products. An assembly process generally includes part positioning (or mating) followed by part joining. Part positioning can be accomplished using fixtures or robots. Part joining methods include mechanical fasteners, shrink and expansion fits, welding, and adhesives. Because an assembly process is the place where quality variation from the individual components could accumulate, it is critical to monitor and diagnose assembly and joining problems quickly and effectively.

This chapter provides an overview of various approaches available for monitoring assembly and joining processes, in particular, resistance spot welding and arc welding processes; Section 8.1 describes techniques in the monitoring of assembly processes using examples from automotive body assembly processes; Section 8.2 describes the monitoring and control of resistance spot-welding processes; and Section 8.3 presents techniques in the monitoring and control of gas metal arc welding processes.

8.1 Assembly Processes

There are two types of assembly processes (Mantripragada, 1998). Type I assemblies are comprised of machined or molded parts that have their matting features fully defined by their respective fabrication processes prior to assembly, for example, the insertion of a peg into a hole. Mating of part features is the main function of the assembly process. Type II assemblies are those where some or all of the assembly features and/or their relative locations are defined during assembly. These types of assembly processes include, for example, automotive and aircraft body assemblies where part mating is accomplished using fixtures during the assembly process.

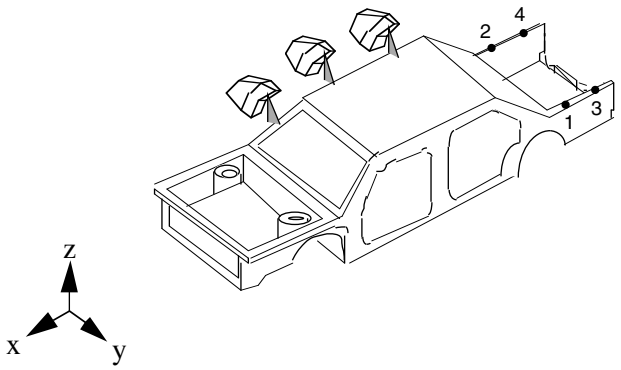

FIGURE 8.1 A schematic of an optical coordinate measuring machine checking body dimensions.

Monitoring of an assembly process can be accomplished by either directly monitoring the quality characteristics of the assembled products (i.e., key product characteristics or KPCs), or monitoring the processes characteristics that control the assembly process (key control characteristics or KCCs), i.e., fixtures and welding machines. Examples of KPC monitoring include inspection of an assembly on coordinate measuring machines. In automotive body assembly, the KPCs in a car body are the sizes and shapes of the openings. Figure 8.1 shows schematically an in-line optical coordinate measuring machine that is checking the dimensions of a car body assembly.

8.1.1 Monitoring of KPCs

In automotive body assembly, the critical KPCs are the sizes and shapes of the body openings, e.g., doors, trunk opening, etc. Their sizes and shapes influence the downstream panel fitting processes, which, in turn, influence the quality and functionality of the final vehicle. For example, width and straightness are the critical product characteristics for the trunk opening. The indices for the width and straightness of the decklid opening are defined as (Roan and Hu, 1994):

$$I_1 = y_1 + y_2,\ I_2 = y_3 + y_4$$

$$I_3 = y_1 - y_3,\ I_4 = y_2 - y_4$$

where $I_1$and I_2 are width indices, I_3 and I_4 are straightness indices, and y_is are the measured deviations from design nominal dimensions. Because multiple product characteristics are to be monitored at the same time, the simultaneous confidence interval (Johnson & Wichern, 1992) approach can be used to establish control limits for the KPCs.

8.1.2 Monitoring of KCCs

As mentioned before, an assembly process can be monitored using the key control characteristics, such as the fixturing and joining processes. Monitoring the torque in a fastening operation provides such a direct approach to assembly monitoring. However, there are situations in which process measurements are not readily available. In such a case, when only the product characteristics are measured, various transformation techniques can be used to relate KPCs to KCCs. For example, principal component analysis can be used to relate dimensional measurements on automotive bodies to various fixturing faults (Hu and Wu, 1992; Ceglarek and Shi, 1996), then process monitoring can be accomplished using the resulting principal components.

The basic idea behind principal component analysis is to find the interrelationship between variables by taking the combination of them to produce uncorrelated variables. The principal components, z_i, are represented as linear combinations of the n original correlated variables, y_i, as

$$\begin{Bmatrix} z_1 \\ z_2 \\ \vdots \\ z_n \end{Bmatrix} = \begin{bmatrix} a_{11} & a_{12} & \cdots & a_{1n} \\ a_{21} & a_{22} & \cdots & a_{2n} \\ . & . & \cdots & . \\ a_{n1} & & & a_{nn} \end{bmatrix} \begin{Bmatrix} y_1 \\ y_2 \\ \vdots \\ y_n \end{Bmatrix}$$

where the a_{ij} are the j-th elements of the i-th eigenvectors of the covariance matrix C of the original correlated variable y_i.

An example of assembly monitoring using principal components is shown in Figure 8.2. Here measurements are made on the cross-car deviation of the roof after assembly. Figure 8.2(a) shows these dimensions. Figure 8.2(b) shows the principal components, z_i's. Because z_i's are not correlated with each other, standard process control charts, such as x-bar and R charts, can be used as tools for monitoring (DeVor et al., 1992).

8.2 Monitoring and Control of Resistance Welding Process

The resistance welding process is a very popular joining technique used in the manufacture of such items as automobiles, furniture, and appliances. For example, in a typical steel auto body, there are from 3000 to 5000 weld spots. Because of the extensive use of resistance spot welding, even a small improvement would bring significant economic benefits. This potential payoff has attracted a significant amount of research in both the resistance spot-welding field in general and the specific field of resistance spot-welding monitoring and control.

Resistance welding is the process of welding two or more metal parts together in a localized area by applying heat and pressure. The heat is provided by the resistance furnished by the metal parts to the flow of current through the electrode tips. The pressure is also provided by these same electrodes through pneumatic cylinders or servo drives. The schematics of a resistance welding machine are shown in Figure 8.3.

Many models of resistance spot welding were based on two coupled partial differential equations (Matushita, 1993): an electrical equation

$$\nabla \cdot \left(\frac{1}{\rho_1} \nabla V \right) = 0$$

and a thermal equation

$$C\sigma \frac{\partial T}{\partial t} = \nabla \cdot (K \nabla T) + \rho_2 \delta^2$$

where $\rho 1$ is the electrical resistivity of the workpiece, V is the electrical potential, K is the thermal conductivity, ∇ is the gradient, C is the specific heat, σ is the workpiece mass density, and δ is the current density. To handle the complexity of solving these partial differential equations, most researchers have resorted to finite difference methods or finite elements methods. Unfortunately, these models and methods are not computable on-line, therefore, not suitable for on-line monitoring and control.

The difficulty of generating simple dynamic models from the first principles has led researchers to use ad hoc techniques for monitoring and control. Because weld quality, whether defined as a weld attribute such as butt diameters from peel test, or strength, such as tensile strength of the weld, is not directly measurable, identifying variables with a high correlation with nugget size would be desirable. Variables studied so far include thermal emission, ultrasound, acoustic emission, thermal expansion, temperature, voltage, current, energy, resistance, force, and residual stress. The most commonly used variables are current (I), dynamic resistance (DR), and electrode displacement (D).

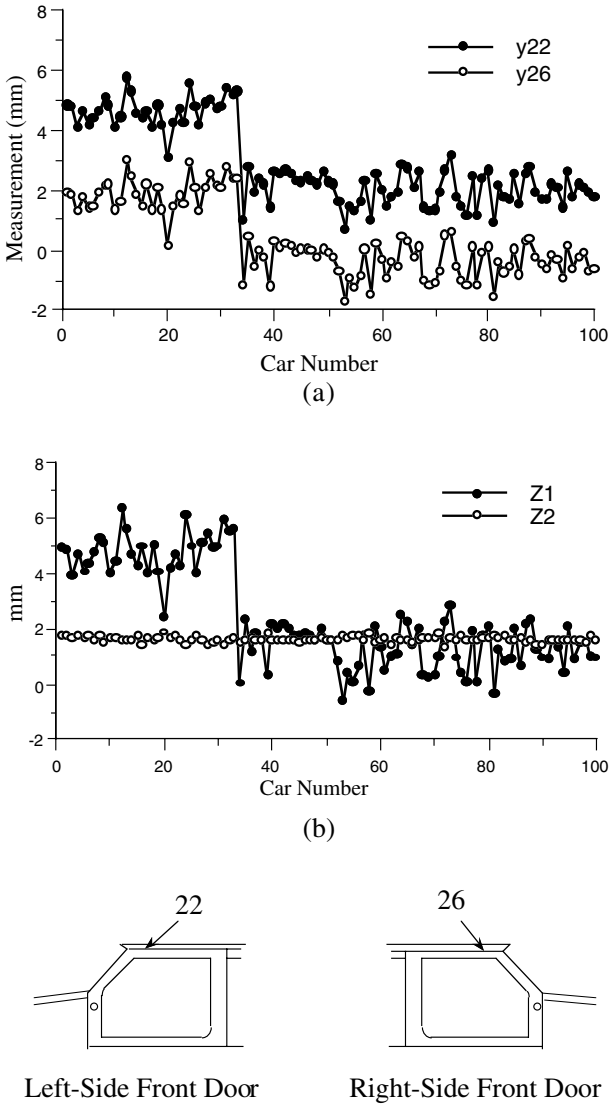

FIGURE 8.2 Monitoring of principal components.

8.2.1 Monitoring

The possible importance of electrode head displacement was recognized early in a 1942 U.K. patent. Waller (1964) reasoned that weld quality was related to maximum displacement and thus took maximum displacement as a sign of weld quality. Needham proposed a controller that shuts off the current when the weld displacement reaches approximately 80% of a predetermined maximum value. In other words, it is a closed-loop weld schedule around the displacement measurement. Jantoa (1975) suggested using a zero rate of expansion as the signal that a complete weld had been made. Kuchar et al. (1982) use a finite element model (FEM) model to create ideal electrode displacement curves and then design a classical controller to track them. After this, several research groups (Cho et al., 1985, Wood et al., 1985, Chang et al., 1989) also studied tracking control of displacement signals. Adaptive control techniques have also been studied (Chang et al., 1989, Haefner et al., 1991).

A displacement curve as shown in Figure 8.4 has been suggested by various researchers (Gedeon et al., 1987). Here the displacement curve is divided into different regions and process monitoring

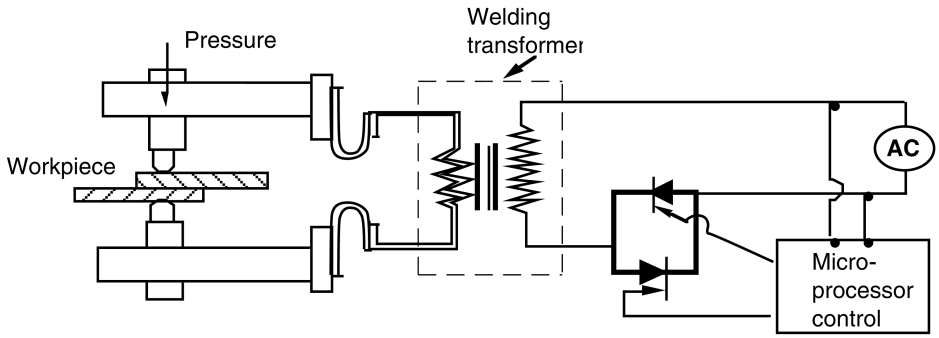

FIGURE 8.3 Resistance welding process.

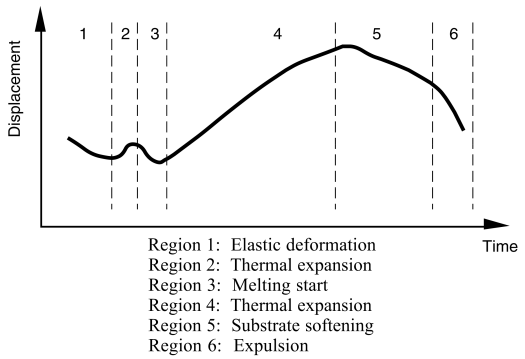

FIGURE 8.4 Monitoring of resistance welding process using electrode displacement.

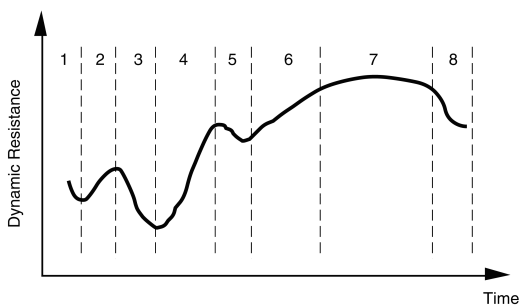

FIGURE 8.5 Monitoring of resistance welding process using dynamic resistance.

is accomplished by detecting changes of the curve from region to region. However, the magnitude of the displacement curve will be modulated by machine stiffness and weld force. Therefore, there is no ideal displacement curve unless the welding force is maintained at a constant level and the curve is calibrated for each machine.

The rationale behind using dynamic resistance as a feedback signal has taken a very similar approach to that of electrode displacement. The dynamic resistance curves provide excellent information and were believed to be much easier to instrument than force or displacement (Figure 8.5). However, for coated steels, it was difficult to relate dynamic resistance with nugget information. One of the early dynamic resistance-based controllers was presented by Towey (1968).

The idea was that the resistance drop was related to the size of the nugget and thus, by looking for a predetermined resistance drop, they could get the desired size nugget. Dickinson et al. (1980) divided the dynamic resistance curve into the following stages: surface breakdown, asperity collapse, heating of the workpieces, molten nugget formation, nugget growth, and mechanical collapse. In 1987, Gould found that neither poor fit-up nor use of sealer at the faying surface adversely affected the resistance-based control algorithms.

Monitoring systems based on other indirect signals also have been developed. For example, one of the earliest acoustic/ultrasonic monitoring systems was devised by Burbank et al. in 1965. Vahavilos (1981) studied acoustic emission as a feedback signal for weld quality control. While good performance was claimed, this controller appears to have been unsuccessful in production environments. The biggest obstacles seem to be the availability of sensors suitable for a shop-floor environment, and lack of a real-time signal-processing device that can handle the huge amount of data coming from the sensors.

Currently, process monitoring for resistance spot welding has focused on a multivariate approach. For example, Hao, Osman, Boomer, and Newton studied the characterization of resistance spot welding of aluminum. Both single-phase alternating current (AC) and medium-frequency direct current (MFDC) are used. From the recorded weld data file, a large number of features are extracted to monitor the nugget growth. Li et al. (1998) used principal component analysis to extract features and then neural networks to classify fault and predict nugget growth.

8.2.2 Control

Two major difficulties exist with spot-welding control: First, there is no direct way to sense nugget diameter (or strength) in real time. All the variables that can be sensed in real time have been shown to be at best weakly linked to nugget diameter and strength. Many of the available sensors are also found to be unsuitable under a production environment. Second, a sufficiently good model of the process, in a form useful for control design, is difficult to develop.

To circumvent the first difficulty, two control approaches are usually taken: (1) open-loop control (weld schedule, table lookup); and (2) feedback and control of indirect welding variables such as current, displacement, force, acoustic emission, etc. In the first approach, the system is vulnerable to any external disturbances (e.g., power fluctuation, poor fit-up, etc.). In the second approach, the system is vulnerable to any external disturbances whose effect on nugget size/strength is undetectable from the feedback signal. The second approach seems to be more promising for generating consistent welds if we can identify the right signal/sensor to close the loop.

Current was used in the earliest attempts as a signal for resistance spot welding (RSW) control for two main reasons: First, there is a close relationship between current and total energy input to the welding process. Second, current is directly controllable and is often used as the control input. The assumption behind current control is that if the resistance across the two electrodes is constant, then controlling electrical current (I) will provide direct control of the heat generated. Later on, it was realized that resistance between electrodes (R) is not constant (it changes with temperature, pressure, etc.). Variation to current control was adapted. For example, current density (current divided by electrode face area) was attempted to compensate for electrode wear. As an electrode wears, a current stepper in the weld control system will increase the current to try to maintain constant current density.

The paper by Kuchar (1982) discusses a closed-loop multivariable control system using an axisymmetric finite element model. The outputs from the FEM model are predicted nugget size and corresponding electrode displacement for quality welds. Measured electrode displacement is then compared with the ideal displacement curve and the error is used for feedback control. The controller adjusts the electrode force, current, and voltage to bring the actual displacement close to the ideal displacement curve. Tsai et al. (1991) also studied the correlation between the expansion displacements among the electrodes during welding to the weld nugget quality.

Haefner, Carey, Bernstein, Overton, and D'Andrea (Haefner et al., 1991) developed a system incorporating adaptive control technology for the process. This paper relates thermal growth to nugget formation by deriving the thermal growth from the electrode displacement measurement. This real-time adaptive strategy adjusts for long-term electrode wear and provides a short-term weld-to-weld control to compensate for fit-up and surface oxide variations. Schumacher et al. (1984) developed an adaptive control system that could weld different low-carbon and high-strength steels, or a series of different welds in the same steel.

Recently, the research focus on spot-welding control seems to have shifted toward intelligent control, or more specifically, neural network/fuzzy logic/expert system-based control systems. One of the unique features of these systems, compared with traditional control design methods, is that they generally do not require an explicit system model, and the control algorithm can be based on rules or other forms of knowledge. Examples include Jou et al. (1994) and Shriver et al. (1998). Because these techniques are relatively new, most of the proposed methods were not implemented as control algorithms. They either involve proof-of-concept type of study, or are designed to generate weld parameter suggestions, instead of controlling the weld process directly.

8.3 Monitoring and Control of Arc Welding Processes

Welding processes often encounter disturbances that effectively change the process outputs, resulting in a weld of undesirable characteristics. Such disturbances may include thermal distortion, workpiece fit-up, geometrical variations in workpieces, robot motion errors, and the effects of fixturing equipment. To achieve the desired weld characteristics while the process is subjected to disturbances, it is necessary to use feedback control. The three principal stages of process control involve modeling, sensing, and control (Cook et al., 1989; Kannatey-Asibu, Jr., 1997).

At the core of feedback control are the process inputs and outputs. The primary inputs in the case of gas metal arc welding, for example, are the arc current/arc voltage, traverse velocity (welding speed), and electrode wire feed rate (Cook, 1980; Dornfeld et al., 1982). The secondary inputs include shielding gas flow, torch positioning and orientation, torch weaving or oscillation, and mode of metal transfer. Non-manipulatable inputs include workpiece and electrode material properties, workpiece geometry, and joint configuration. The primary outputs are usually difficult to measure in real time, i.e., while the process is going on, and without destroying the part, while the secondary outputs are more easily measured on-line, but not after the process. The primary outputs include penetration, bead width, reinforcement (collectively, the bead cross-sectional area), hardness, strength, microstructure, residual stresses, and discontinuities (cracks, inclusions, porosity, etc.). The secondary outputs include peak temperatures (temperature distribution), cooling rate, arc length, acoustic emission, arc geometry, arc motion, and pool motion.

In this section, we focus on modeling and sensing of arc welding processes for control, even though control schemes are discussed in other chapters, and with specific emphasis on welding processes in Cook (1989), Suzuki et al. (1991), and Tomizuka et al. (1980). The discussion starts with modeling for feedback control of arc length followed by models for control of weld bead geometry and weld material properties. Various techniques for monitoring the welding process are then outlined.

8.3.1 Modeling for Arc Length Control

Control of arc length is useful for wire feed welding systems such as gas metal arc welding. Arc length variations for these systems can result from variations in power line voltage, groove geometry, etc. and can affect porosity and other forms of discontinuity. Feedback control of arc length using wire feed as input normally involves a constant current power source. With such a power source, the system is not self-regulatory, and therefore significant variations in arc length can occur unless it is under closed-loop control.

The simplest model of arc length dynamics describing the characteristics of the gas metal arc welding system is based on the assumption that the rate of correction of the welding wire tip is proportional to displacement from its equilibrium position or operating point. In other words, the rate of change of arc length is proportional to the change in arc length and is expressed (Muller, Greene, Rothschild, 1951) as

$$\frac{dl}{dt} + \frac{1}{\tau} l = 0 \tag{8.1}$$

where l = change in arc length, and τ = proportionality constant.

Using the melting rate relationship (Lesnewich, 1958; Halmoy, 1979; 1981), a more complete form of Equation (8.1) which incorporates the control input is given (Kannatey-Asibu, Jr., 1987; Wu and Richardson, 1989) by

$$\frac{dl}{dt} = -K_5 l - r\omega \tag{8.2}$$

where $K_5 = K_0\, mn$, m = arc voltage — arc length characteristics slope, n = absolute value of the inverse of the power source characteristics slope, K_0 = constant, r = transmission ratio from the wire drive motor to the wire speed, l = arc length, t = time, and ω = drive motor rotational speed.

The corresponding transfer function is

$$L(S) = -\frac{K_w}{\tau_w s + 1} \Omega(S) \tag{8.3}$$

where $\tau_w = 1/K_5$ is the weld process time constant, $K_w = r/K_5$ is the weld process gain, and L(S) and Ω(S) are the Laplace transforms of the arc length and motor angular speed, respectively.

If the wire-feed drive motor is modeled as a first-order system, then the overall system transfer function becomes

$$L(S) = -\frac{K_w K_m}{(\tau_w S + 1)(\tau_m S + 1)} E_m(S) \tag{8.4}$$

where E_m is the input voltage to the drive motor, τ_m the motor time constant, and K_{m} the motor gain.

8.3.2 Weld Bead Geometry Control

One of the important characteristics of a weldment is the geometry of the weld bead as defined by its cross-sectional area, but in simpler terms the bead width and depth of penetration. The models developed in this and the next section may also be applicable to conduction mode laser welding.

The dynamics of the weld pool for full penetration autogenous welding, i.e., when there is no filler metal being added, can be obtained by considering the idealized configuration when the weld pool is assumed to be isothermal and at the melting point of the material (Hardt et al., 1985; Bates and Hardt, 1985). The pool walls are assumed to be vertical, conduction heat transfer is considered to be the principal mode, and the dynamics of weld pool volume resulting from melting are considered to overshadow thermal dynamics of the solid material. For an idealized cylindrical geometry, the heat balance for the system is

$$Q_{in} = Q_c + \rho L_h \frac{dV_0}{dt} \tag{8.5}$$

where Q_{in} is the net heat input from the source to the weld pool and is given by ηEI for arc welding; Q_c is the heat flow by conduction from the weld pool to the base material; ρ is the density of the molten pool; L_h the latent heat of fusion; V_0 the pool volume; η heat transfer efficiency; E arc voltage; and I the welding current.

Using Fourier's law, the conduction term can be expressed as

$$Q_c = -2\pi khr\frac{dT}{dr} \tag{8.6}$$

where k is the thermal conductivity, h the plate thickness, r the pool radius, and T is the temperature. Expressing the volume V_0 in terms of the radius and height of the pool, Equation (8.5) then reduces to

$$Q_{in} = 2\pi\rho L_h hr\frac{dr}{dt} - 2\pi khr\frac{dT}{dr} \tag{8.7}$$

This is a nonlinear equation for the dynamics of the pool radius. In this form, the equation is not suitable for use in simple feedback control. A form more suitable for simple control can be obtained by lumping variables together as follows:

$$\eta EI = A(r,h)\frac{dr}{dt} + B\left(k,h,\frac{dT}{dr}\right)r \tag{8.8}$$

The result is a nonlinear first-order model of the process. However, if the parameters A and B are assumed to be constant, then the Laplace transform of the equation can be taken to obtain the following transfer function of the system:

$$\frac{R(S)}{I(S)} = \frac{K}{\tau_p S + 1} \tag{8.9}$$

where $K = hE/B$ is the process gain, $\tau_p = A/B$ is the process time constant, and $R(S)$ and $I(S)$ are the Laplace transforms of the pool radius and welding current, respectively.

8.3.3 Weld Material Properties

Another primary output of the welding process is the microstructure, which determines the weld material properties. Again, we are faced with the problem that this output is not directly measurable in real time, i.e., it is unobservable. Thus, feedback control that involves direct measurement of this parameter as an output cannot be implemented. However, closed-loop control of the temperature field, along with an open-loop microstructure and material properties output would significantly mitigate the impact of disturbances.

In this regard, the appropriate inputs for the process are the heat input Q_{in}, and traverse velocity, V. The outputs are the bead cross-sectional area NS, heat-affected zone size HAZ, and centerline cooling rate CR.

8.3.3.1 Bead Size

The dynamic relationship between the bead size NS and either the heat input Q_{in} or welding velocity V is modeled as first order (Doumanidis and Hardt, 1989):

$$\frac{NS(S)}{V(S)} = \frac{K_a}{\tau_a S + 1} \tag{8.10}$$

8.3.3.2 Heat-Affected Zone Size

Because the heat-affected zone is given by the difference between two isotherms, the solidification temperature T_s (for a pure material) and the temperature at which a phase change occurs T_h, with each being described by a first-order behavior, the heat-affected zone is expected to exhibit a non-minimum phase second-order behavior. Thus,

$$\frac{HAZ(S)}{Q_{in}(S)} = \frac{K_1}{\tau_1 S+1} - \frac{K_2}{\tau_2 S+1} = \frac{K_b(\tau_b S+1)}{(\tau_1 S+1)(\tau_2 S+1)} \tag{8.11}$$

8.3.3.3 Cooling Rate

The centerline cooling rate response to a step change in either Q_{in} or V is best described by an overdamped second-order behavior:

$$\frac{CR(S)}{Q_{in}(S)} = \frac{K_c}{(\tau_\alpha S+1)(\tau_\beta S+1)} \tag{8.12}$$

Having outlined some of the basic models that constitute the basis for weld process control, we now discuss some of the more common sensor systems for monitoring process outputs.

8.3.4 Monitoring of Arc Welding and Laser Welding

The hostile nature of the process environment (high temperatures and spatter) presents difficulties in the development of reliable sensors. The principal parameters that need to be monitored during laser welding, for example, include the weld pool geometry (width and penetration); discontinuities (cracking, porosity, etc.); microstructure (strength); residual stresses; peak temperatures; and cooling rates. Among the most commonly used sensors are acoustic emission, audible sound (acoustic sensing), infrared/ultraviolet detectors, and optical (vision) sensors. A brief overview of commercially available systems is presented first, followed by an outline of each of the principal sensor systems.

8.3.4.1 Commercially Available Systems

Most of the systems currently available commercially in the United States for monitoring welding processes maintain process inputs such as current, voltage, wire feed rate (in the case of arc welding), and gas flow rate within some desirable range. Two of the key systems include the Computer Weld Technology (formerly CRC-Evans) Arc Data Monitor (ADM) and Jetline Engineering's Archcon Weld Monitor. The LWM 900 is marketed by JURCA Optoelektronik in Germany, for monitoring CO_2 laser welding processes. As opposed to the ADM and Archon systems, the LWM 900 indirectly monitors the process output by detecting the ultraviolet and infrared radiation emitted by the welding plasma and glowing metal spatter, respectively. It analyzes the amplitude and frequency of the detected signals. The PMS10 plasma monitoring system by Thyssen also detects plasma radiation and analyzes it by considering the plasma interrupts that are grouped into three categories, plasma flashes grouped into two categories, and average plasma intensity. The groupings for the first two cases are based on the duration of the signal. These parameters are then used to detect porosity formation and incomplete penetration.

8.3.4.2 Acoustic Emission

One sensor type that has been extensively investigated for weld process monitoring is acoustic emission (AE). AE refers to stress waves that are generated as a result of the rapid release of elastic strain energy within a material due to a rearrangement of its internal structure. It is also sometimes referred to as stress wave emission. The resulting stress waves propagate through the structure and

produce small displacements on the surface of the structure. These are detected by sensors which convert the displacements into electrical signals. AE is an active phenomenon, because it is generated by the process under investigation. In addition, AE signals are well suited for real-time or continuous monitoring because they are generated while the phenomenon is undergoing change. Two types of transducers are normally used for AE signal detection: piezoelectric transducers and capacitive transducers.

Investigations into AE generation during electron beam welding indicate that an increase in the intensity of energy input increases the AE signal intensity (Dickhaut and Eisenblatter, 1975). Continuous signals have been associated with smooth weld beads, while burst signals apparently correlate with surface markings on nonuniform weld beads. Defect-related signals, especially cracks, have been found to be of greater amplitude than the continuous AE signals (Fang et al., 1996; Jolly, 1969; Wehrmeister, 1977). However, the presence of other undesired signal sources made the detection of the actual crack signals rather difficult (Prine, 1978). Most of the difficulty was caused by the method of signal analysis used at the time, the ring-down count. In recent years, signal processing of acoustic emission signals has been extended from traditional count and count rate analyses to the more reliable pattern recognition analysis that also enables different signal sources to be identified (Liu and Kannatey-Asibu, 1990).

Acoustic emission, too, has found application in the location of the focal point during laser welding, being maximum when the focal point coincides with the work surface (Orlick et al., 1991), and also in laser spot welding (Hamann et al., 1989; Weeter and Albright, 1987).

Precautions that need to be taken when applying conventional AE instrumentation to welding include (a) protecting the transducer from the high temperatures of welding environments and providing a highly reliable acoustic contact between the transducer and the structure; (b) positioning the transducer with respect to the material being welded and the source location; and (c) protecting the instrumentation from electromagnetic interferences resulting from arc welding equipment (Nechaev, 1978).

8.3.4.3 Audible Sound

Most manufacturing processes naturally emit sound, and an experienced human operator can use these operational sounds to determine whether or not the process is functioning normally. This indicates that the sound emitted by the process contains information that can be used to monitor the system. Audible sound sensors detect low-frequency (5 to 20 kHz) signals generated during processing (Mombo-Caristan et al., 1991), and involve microphones directed toward the process area. An advantage of audible sound monitoring is that it is noncontact, and also reduces the risk of instrumentation damage. Another advantage is the relatively lower frequency range, which makes it easier to digitize and analyze the signals.

Various methods have been investigated for analyzing sound signals generated during welding. These include statistical approaches which show that there is a narrow band of audible sound emission near 4.5 kHz for good welds, with no narrow band being observed for poor welds, but where the spectrum spreads out with a significantly lower amplitude (Gu and Duley, 1994, 1996). Neural network and linear discriminant functions also have been used to monitor on-line arc welding quality and classify the signals as acceptable or unacceptable (Matteson et al., 1993). Time-frequency analysis of audible sound signals emanating from the weld also indicates that the spectrum of a good weld can be differentiated from the spectrum of a bad weld (Farson et al., 1991, 1996).

8.3.4.4 Acoustic Nozzle and Acoustic Mirror

Airborne signals sensed by mounting a piezoelectric transducer on the focusing optic have been compared with AE signals from a piezoelectric transducer mounted on the workpiece. The results indicate airborne signals are capable of monitoring weld defects (Hamann et al., 1989; Jon, 1985). Signals from the laser welding process have also been monitored using the acoustic nozzle and the acoustic mirror (Li and Steen, 1992; Steen and Weerasinghe, 1986). With the acoustic nozzle, the

transducer is mounted on the focusing assembly nozzle, while with the acoustic mirror the transducer is mounted on the reflecting mirror. Experimental results indicate that signal strength is a function of penetration depth, incident power, and plasma density. Additional results indicate that signal amplitudes increase dramatically when the keyhole forms.

8.3.4.5 Infrared/Ultraviolet Sensors

The infrared-ultraviolet (IR/UV) detection technique analyzes radiation emitted from the process zone in two wavelength bands: the infrared band in which most of the radiation from the hot material is considered to be concentrated, and the ultraviolet band in which the plasma radiation is considered to be concentrated (Chen et al., 1991; Lewis and Dixon, 1985). A typical sensor used for infrared radiation is a germanium photodiode fitted with a silicon filter having a spectral range from 1.0 to 1.9 mm. The ultraviolet radiation may be measured with a gallium phosphide (GaP) photodiode with a spectral range from 0.19 to 0.52 mm. Even though the signal intensity is generally observed to depend on the viewing distance, its characteristics are found to be independent of the arrangement used when viewing at two fixed wavebands. Both the ultraviolet and infrared signal intensities, however, increase with laser power, while increasing shielding gas flow rate reduces the signal intensities, probably due to a reduction in plasma volume.

Spatial temperature gradients in the vicinity of the weld pool can be detected using infrared thermography. An ideal weld should result in regular and repeatable patterns of the temperature gradients. Imperfections in the welding process, however, result in a discernible change in the thermal profiles. Chin et al. (1983, 1989), Boillot et al. (1985), Khan et al. (1984), and Nishar et al. (1994) showed that the average weld pool diameter can be obtained from a line scan across the center of the pool profile, and is given by the inflections around the peak temperature. When the heat source is shifted to one side of the joint center, the thermal image becomes distorted in shape, consisting then of halfmoon shapes. This asymmetrical temperature distribution is caused by the excess energy which is deposited on one side of the joint relative to the other, and the contact resistance at the joint, which reduces heat flow across the joint, resulting in higher temperatures on the side with excess energy. The heat source can then be moved in the appropriate direction until the two radii are equal. A variation in the seam also causes a shift in the shapes of the isotherms.

In addition to being used for joint tracking, the temperature isotherms can also be used to identify geometrical variations encountered in the welding process such as in the joint opening and mismatches. For example, a variation in the joint opening causes an indentation in the isothermal lines corresponding to a decrease from the peak temperatures of the metal surrounding the opening. Impurities in the weld pool appear as cold spots in the thermograms.

8.3.4.6 Weld Pool Oscillation

The weld pool, being a fluid system, oscillates when subjected to appropriate excitation, and the nature of the oscillation is determined by the pool's geometric configuration as well as its physical properties (Renwick and Richardson, 1983; Sorensen and Eagar, 1990; Xiao and den Ouden, 1993). For a stationary weld pool of infinite depth, the natural frequency of the pool is related to its geometry and properties if the fluid is assumed to be inviscid and incompressible, with flow being irrotational:

$$\omega_n^2 = \frac{7.66g}{W} + \frac{4.49\gamma}{W^3\rho}$$

while that of a pool of finite depth D is

$$\omega_n^2 = \left[\frac{7.66g}{W} + \frac{4.49\gamma}{W^3\rho}\right]\tanh\left(\frac{7.66D}{W}\right)$$

where g = acceleration due to gravity, γ = surface tension, W = width of the weld pool, and ρ = density of the weld pool. This may be used to characterize arc and conduction-mode laser welding systems.

8.3.4.7 Optical Sensing

Optical sensing (vision) is often used for monitoring weld pool geometry, observing flow on the free pool surface, and chevron formation during welding. It is also useful for monitoring the kerf size during laser cutting and laser material interactions in general (Denney and Metzbower, 1991).

The basic components of an optical sensing system include the sensor, illumination source, object, transmission elements, and finally the processor. The sensing elements may be, for example, silicon photodiodes or lateral effect diodes. The lateral effect diode behaves like a resistor with a photogenerated current induced along its length by an incident light. The detector elements are normally very light sensitive, and thus may saturate easily. Attenuation of the signal is often necessary, and caution needs to be exercised in this regard because improper attenuation can introduce distortion and interference effects. The wavelength response is typical of the spectral response of the silicon which falls in the range 0.19 to 1.10 mm.

In the case of welding, for example, the sensed objects include the joint to be welded, weld pool, under bead, and bead surface. Some of the problems associated with optical sensing include the extreme brightness of the plasma plume compared to that of the molten pool (high contrast), and dependence of the intensity on processing conditions. Spatter, fumes, and flux also may obscure the object to some extent. As a result of these problems, separate illumination is often used to counteract the effect of plasma plume illumination, maintain a stable intensity that is appropriate for the sensor, enhance contrast, and provide a brightness level that is suitable for the sensor. This increases the system resolution. The separate illumination may be in the form of either structured light or general illumination, i.e., nonstructured light. A structured light is a pattern of lines or a grid of light projected onto the object to help provide information on the three-dimensional shape of the object based on the apparent distortion of the pattern.

The general illumination could come from an auxiliary high-intensity light source. One application of general illumination would involve lighting the object with a narrow bandwidth laser beam, with the beam bandwidth selected to be in the region where, based on the spectral characteristics of the detector, the detector's sensitivity is high. All light on the detector is then filtered except for the narrow bandwidth of the auxiliary beam, thereby subduing the effect of the bright light from the plume. An enhancement of this technique involves the use of both diffused and focused light (Voelkel and Mazumder, 1990).

There are two main forms of optical sensing systems: linear array systems and two-dimensional array systems. The linear systems may consist of a column of, for instance, up to 2048 pixels or individual sensing elements in a line, while the two-dimensional system may have 500×500 elements.

One principal advantage of the linear array sensor is the rapid processing of information. The resolution is limited by the size of the field of view and the spacing of the sensing elements. Moving the sensor along the joint provides information on the joint profile. Periodic scanning of the array yields the light intensity detected by each sensing element. Objects of interest can be identified using various techniques, but in the simplest case, a threshold light intensity may be defined for the object, such as the edge of a weld pool, and used to identify the pool edges. A line scan camera has been used to measure the width of the weld puddle (Vroman and Brandt, 1976; Nomura et al., 1976).

The two-dimensional array detector monitors a sizeable area simultaneously, and is thus suited for two-dimensional objects such as the weld pool. The sensor in this case is normally a solid-state video camera with an array say, 500×500 charge injection device or charge coupled device light sensitive elements. The output of each element or pixel may be an 8-bit digitized video. The output from the camera may be immediately dumped into a memory buffer for analysis.

The pool width may be identified by analyzing the output of a row of elements located across the weld pool. The pool area will require the entire two-dimensional image. The output may be processed by averaging each pixel's signal with a given number of pixels on either side. The waveform may then be numerically differentiated by finding the difference between each adjoining pixel, and again averaging the resulting signal. From this processed signal, the weld pool edges would be given, for example, by the second zero crossings (Kovacevic et al., 1995; Richardson et al., 1982).

For viewing the pool and/or the joint, the camera may be positioned at any desirable location, but a convenient configuration involves having the camera's optical axis coincident with the beam axis, providing an image of the weld pool and surrounding area (Richardson et al., 1984).

8.3.4.8 Multi-Sensor Systems

In recent years multi-sensor systems have been investigated for monitoring manufacturing processes. Utilizing multi-sensor integration incorporates the advantages of different sensors into one system. Furthermore, incorporating modularity permits the selection of the combination of sensors most appropriate for a particular application. An integrated system consisting of an acoustic mirror for back reflection, acoustic nozzle for airborne emissions, plasma charge sensor for plasma monitoring, and a dual wavelength infrared and ultraviolet sensing of the weld region has been investigated for laser welding. (Steen, 1992) The results indicate that the acoustic mirror, acoustic nozzle, and plasma charge sensor can monitor keyhole formation while the infrared/ultraviolet sensor can monitor the temperature and size of the weld pool and the stability of the keyhole. Other sensor combinations have been investigated (Parthasarathi et al., 1992).

8.3.4.9 Seam Tracking

A weld-seam tracking system that senses the arc voltage (GTAW) or current (GMAW) while oscillating the welding torch from one sidewall extremity of the joint to the other has been developed using the melting rate equation and relationships that exist between the arc voltage, current, and torch-to-work spacing, Cook (1983). Seam tracking also can be implemented using infrared and vision systems.

References

Bates, B. E. and Hardt, D.E., 1985, A real-time calibrated thermal model for closed-loop weld bead geometry control, *ASME Journal of Dynamic Systems Measuremetn and Control*, 107, 25–33.

Boillot, J. P., Cielo, P., Begin, G., Michel, C., Lessard, M., Fafard, P., Villemure, D., 1985, Adaptive welding by fiber optic thermographic sensing: An analysis of thermal and instrumental considerations, *Welding Journal*, 64, 209s–217s.

Ceglarek, D., and Shi, J., 1996, Fixture failure diagnosis for autobody assembly using pattern recognition, *ASME Journal of Engineering for Industry,* 118, 1, 55–66.

Chang, H. S. and Cho, H. S., 1989, An interactive learning control system for resistance spot welding process, *Transactions of ASME*, 111, 129–135.

Chen, H., Li, L., Brookfield, D., Williams, K., and Steen, W., 1991, Laser process monitoring with dual wavelength optical sensors, *ICALEO'91*, 113–122.

Chin, B. A., Madsen, N. H., and Goodling, J. S., 1983, Infrared thermography for sensing the arc welding process, *Welding Journal*, 62, 227s–234s.

Chin, B. A., Nagarajan, S. and Chen, W. H., 1989, Infrared sensing for adaptive arc welding, *Welding Journal*, 68, 462s–466s.

Cho, H. S., and Chun, D. W., 1985, A microprocessor-based electrode movement controller for spot weld quality assurance, *IEEE Transactions on Industrial Electronics*, IEEE-32, No. 3.

Cook, G.E., 1980, Feedback control of process variables in arc welding, *Proceedings, 1980 Joint Automatic Control Conference*, San Francisco, CA.

Cook, G. E., 1983, Through-the-Arc Sensing for Arc Welding, *10th NSF Conference on Production Research and Technology*, Detroit, Michigan, 141–151.

Cook, G. E., Anderson, K., and Barrett, R. J., 1989, Feedback and Adaptive Control in Welding, *2nd International Conference on Trends in Welding Research*, Gatlinburg, Tennessee, David, S., and Vitek, J. M., editors, 891–903.

Denney, P. E., and Metzbower, E. A., 1991, Synchronized laser-video camera system study of high power laser material interactions, *ICALEO*, 84–93.

DeVor, R.E., Chang, T., and Sutherland, J., 1992, *Statistical Quality Design and Control, Contemporary Concepts and Methods*, Macmillan, New York.

Dickinson, D. W., Franklin, J. E., and Stanya, A., 1980, Characterization of spot welding behavior by dynamic electrical resistance monitoring, *Welding Journal*, 59(6), 170-s–176-s.

Dickhaut, E. and Eisenblatter, J., 1975, Acoustic emission measurements during electron beam welding of nickel-base alloys, *Journal of Engineering Power Transactions ASME*, 97, 47–52.

Dornfeld, D.A., Tomizuka, M., and Langari, G., 1982, Modeling and adaptive control of arc-welding processes, *Measurement and Control for Batch Manufacturing*, Hardt, D. E., ed., 65–75.

Doumanidis, C., and Hardt, D.E., 1989, A model for in-process control of thermal properties during welding, *ASME Journal of Dynamic Systems, Measurement, and Control*, 111, 40–50.

Fang, C.-K., Kannatey-Asibu, Jr., E., and Barber, J., 1996, Far-field initial response of acoustic emission from cracking in a weldment, *ASME Journal of Manufacturing Science and Engineering*, 119, 281–289.

Farson, D. F., Fang, K. S., and Kern, J., 1991, Intelligent laser welding control, *ICALEO*, 104–112.

Farson, D., Hillsley, K., Sames, J., and Young, R., 1996, Frequency-time characteristics of air-borne signals from laser welds, *Journal of Laser Applications*, 8, 33–42.

Gedeon, S. A., Sorenson, C. D., Ulrich, K. T., and Eagar, T. W., 1987, Measurement of dynamic electrical and mechanical properties of resistance spot welding, *Welding Journal*, 65, 12, 378s–385s.

Gould, J. E., 1987, An examination of nugget development during spot welding, using both experimental and analytical techniques, Welding Research Supplement, *Welding Journal*.

Gu, H., and Duley, W.W., 1994, Acoustic emission and optimized CO2 laser welding of steel sheets, *ICALEO'94*, 79, 77–85.

Gu, H., and Duley, W.W., 1996, Statistical approach to acoustic monitoring of laser welding, *Journal of Physics D: Applied Physics*, 29, 3, 556–560.

Haefner, K., Carey, B., Bernstein, B., Overton, K., and Andrea, M. D., 1991, Real-time adaptive spot welding control, *Journal of Dynamic Systems, Measurement and Control.*

Halmoy, E., 1979, Wire melting rate, droplet temperature, and effective anode melting potential, *Proceedings International Conference on Arc Physics and Weld Pool Behavior,* The Welding Institute, *Cambridge*, 49–57.

Halmoy, E., April 1981, Dynamics of gas metal arc welding, Presented at the American Welding Society Annual Meeting, Cleveland, Ohio.

Hamann, C., Rosen, H.-G., and LaBiger, B., 1989, Acoustic emission and its application to laser spot welding, *SPIE High Power Lasers and Laser Machining Technology*, 1132, 275–281.

Han, Z., Orozco, J., Indacochea, J. E., Chen, C. H., 1989, Resistance spot welding: A heat transfer study, Welding Research Supplement, *Welding Journal.*

Hao, M., Osman, K. A., Boomer, D. R., and Newton, C. J., 1996, Developments in characterization of resistance spot welding of aluminum, *Welding Journal*, 75, 1, 1s–8s.

Hardt, D.E., Garlow, D.A., Weinert, J.B., 1985, A model of full penetration arc-welding for control system design, *ASME Journal for Dynamic Systems, Measurement and Control,* 107, 40–46.

Hu, S. J., and Wu, S. M., 1992, Identifying root causes of variation in automotive body assembly using principal component analysis, *Transactions of NAMRI,* XX, 311–316.

Janota, M., 1975, Control of current and time on the basis of weld nugget, *Proceedings of the IIW.*

Johnson, R. A., and Wichern, D. W., 1992, *Applied Multivariate Statistical Analysis*, Prentice Hall, New York.

Jolly, W. D., 1969, Acoustic emission exposes cracks during welding, *Welding Journal*, 48, 21–27.

Jon, M. C., 1985, Non-contact acoustic emission monitoring of laser beam welding, *Welding Journal*, 64, 43–48.

Jou, M., Messler, R., and Li, C. J., 1994, A fuzzy logic control system for resistance spot welding based on a neural network model, IEEE IAS Meeting, 95CB35862, 1757–1763.

Kannatey-Asibu, Jr., E., 1987, Analysis of the GMAW process for microprocessor control of arc length, *ASME Journal of Engineering for Industry*, 109, 172–176.

Kannatey-Asibu, Jr., E., 1997, Milestone developments in welding and joining processes, *ASME Journal of Manufacturing Science and Engineering,* 119, 801–810.

Khan, M. A., Madsen, N. H., Chin, B. A., Ballard, P., and Lin, T. T., 1984, Infrared thermography as a control for the welding process, *Welding Research Progress*, XXXIX, 2, 28–40.

Kovacevic, R., Zhang, Y. M., and Ruan, S., 1995, Sensing and control of weld pool geometry for automated GTA welding, *ASME Journal of Engineering for Industry*, 117, 210–222.

Kuchar, N. R., Cohen, R. K., Nied, H. A., and Godwin, S. J., Nov. 14, 1982, A closed-loop control system for resistance spot welding, *ASME Winter Annual Meeting.*

Lesnewich, A., August, 1958, Control of melting rate and metal transfer in gas-shielded metal-arc-welding. Part I — Control of electrode melting rate*, The Welding Journal,* 37, 343–353-S.

Lewis, G. K., and Dixon, R. D., 1985, Plasma monitoring of laser beam welds, *Welding Journal*, 64, 49s–54s.

Li, L., and Steen, W. M., 1992, Non-contact acoustic emission monitoring during laser processing, *ICALEO'92*, 719–728.

Li, W., Hu, S. J., and Ni, J., 1998, A model for on-line quality prediction of resistance spot welding, Accepted by *ASME Journal of Manufacturing Science and Engineering.*

Liu, X., and Kannatey-Asibu, Jr., E., 1990, Classification of AE signals for martensite formation from welding, *Welding Journal*, 69, No. 10, 389s–394s.

Mantripragada, R., 1998, Assembly Oriented Design: Concepts, Algorithms and Computational Tools, Ph.D. Thesis, Massachusetts Institute of Technology.

Matteson, A., Morris, R., and Tate, R., 1993, Real-time GMAW quality classification using an artificial neural network with airborne acoustic signals as inputs, *Proceedings of the 12th International Conference on Offshore Mechanics and Arctic Engineering*, III-A, 273–278.

Matushita, 1993, A real time method for contact area calculation, *Proceedings of the IIW.*

Mombo-Caristan, J.-C., Koch, M., and Prange, W., 1991, Seam geometry monitoring for tailored welded blanks, *ICALEO*, 123–132.

Muller, A., Greene, W.J., and Rothschild, G.R., August 1951, Characteristics of the inert-gas-shielded metal-arcs*, The Welding Journal*, 30, 717–727.

Nechaev, V. V., 1978, An acoustic emission transducer for inspecting welding quality, *A translation from Defektoskopiya*, No. 11, 21–27.

Needham, J. C., Benton, D. B., Hannah, M. D., and Newlin, R. G., 1965, Automotive quality control in resistance spot welding mild steel, *Welding Journal,* 44, 4, 168s.

Nied, H. A., 1984, The finite element modeling of the resistance spot welding process, Welding Research Supplement, *Welding Journal.*

Nishar, D. V., Schiano, J. L., Perkins, W. R., and Weber, R. A., 1994, Adaptive control of temperature in arc welding, *IEEE Control Systems,* 94, 4–24.

Nomura, H., Yoshida, T., and Tohno, K., June 1976, Control of weld penetration, *Metal Construction,* 244–246.

Orlick, H., Morgenstern, H., and Meyendorf, N., 1991, Process monitoring in welding and solid state lasers by sound emission analysis, *Welding and Cutting*, 12, 15–18.

Parthasarathi, S., Khan, A.A., and Paul, A.J., 1992, Intelligent laser processing of materials, *ICALEO'92*, 75, 708–718.

Prine, D. W., 1978, A Two Channel Microprocessor Controlled Acoustic Emission Monitor for In-Process Weld Monitoring, *Proceedings 24th Annual ISA Conference*, Albuquerque, New Mexico.

Renwick, R. J., and Richardson, R. W., 1983, Experimental investigation of GTA weld pool oscillations, *Welding Journal*, 62, 29s–35s.

Richardson, R. W., Gutow, A. A., and Rao, S. H., 1982, A vision based system for arc weld pool size control, *Measurement and Control for Batch Manufacturing*, ASME Booklet, Hardt, D.E., Ed., 65–75.

Richardson, R. W., Gutow, D. A., Anderson, R. A., and Farson, D. F., 1984, Coaxial arc weld pool viewing for process monitoring and control, *Welding Journal*, 63, 43s–50s.

Roan, C. and Hu, S. J., July 1994, Multivariate monitoring and classification of dimensional faults for automotive body assembly, *First S. M. Wu Symposium on Manufacturing Sciences*, Beijing, China.

Schumacher, B. W., Cooper, J. C., and Dilay, W., 1984, Resistance spot welding control that automatically selects the welding schedule for different types of steel, *Ford Motor Company Research Report.*

Shriver, J., Hu, S. J., and Peng, H., 1998, Resistance spot welding: A neural network approach to modeling, *Proceedings of the ASME,* MED 8, 201–211.

Sorensen, C. D., and Eagar, T. W., 1990, Measurement of oscillations in partially penetrated weld pools through spectral analysis, *ASME Journal of Dynamic Systems, Measurement and Control*, 112, 463–468.

Steen, W. M., and Weerasinghe, V. M., 1986, In Process Beam Monitoring, *SPIE Laser Processing: Fundamentals, Applications, and Systems Engineering*, 668, 37–44.

Steen, W. M., 1992, Adaptive control of laser material processing, *Proceedings of LAMP*, 1, 439–444.

Suzuki, A., Hardt, D. E., Valavani, L., 1991, Application of adaptive control theory to on-line GTA weld geometry regulation, *ASME Journal of Dynamic Systems, Measurement and Control,* 113, 93–103.

Tomizuka M., Dornfeld, D., and Purcell, M., 1980, Application of microcomputers to automatic weld quality control, *ASME Journal of Dynamic Systems, Measurement and Control,* 102, 62–68.

Towey, M., and Andrews, D. R., October 1968, Instantaneous resistance during spot welding formation as a parameter for an automatic control system, *Welding and Metal Fabrication*, 383–392.

Tsai, C. L., Dai, W. L., Dickinson, D. W., and Papritan, J. C., 1991, Analysis and development of a real-time control methodology in resistance spot welding.

Vahavilos, S.J., Carlos, M.F., and Slykhouse, S.J., 1981, Adaptive spot weld feedback control loop via acoustic emission, *Material Evaluation*, 39, 10, 1057–1060.

Voelkel, D. D., and Mazumder, J., 1990, Visualization and dimensional measurement of the laser weld pool, *ICALEO*, 422–429.

Vroman, A. R., and Brandt, H., 1976, Feedback control of GTA welding using puddle width measurements, *Welding Journal*, 55, 742–749.

Waller, D. N., 1964, Head movement as a means of resistance welding quality control, *British Welding Journal,* 11, 118–122.

Weeter, L., and Albright, C., 1987, The effect of full penetration on laser-induced stress-wave emissions during laser spot welding, *Materials Evaluation*, 45, 353–357.

Wehrmeister, A. E., 1977, Acoustic emission monitoring of multipass submerged-arc welding, *Materials Evaluation*, 35, 45–47.

Wood, R. T., Bauer, L. W., Bedard, J. F., Bernstein, B. M., Czechowski, J., D'Andrea, M. M., and Hogle, R. A., 1985, Closed-loop control systemm for three-phase resistance spot welding, *Welding Journal*, 64, 12, 26–30.

Wu, G.-D., and Richardson, R.W., 1989, The dynamic response of self-regulation of the welding arc, *2nd International Conference on Trends in Welding Research*, Gatlinburg, Tennessee, David, S., and Vitek, J. M., editors, 929–933.

Xiao, Y. H., and den Ouden, G., 1993, Weld pool oscillation during GTA welding of mild steel, *Welding Journal,* 72, 428s–434s.